Journal of Animal Science, 2021, Vol. 99, No. 7, 1–11

doi:10.1093/jas/skab186
Advance Access publication June 9, 2021
Received: 29 April 2021 and **Accepted:** 7 June 2021
Non Ruminant Nutrition

NON RUMINANT NUTRITION

Dietary dimethylglycine sodium salt supplementation improves growth performance, redox status, and skeletal muscle function of intrauterine growth-restricted weaned piglets

Kaiwen Bai,[†] Luyi Jiang,[‡] Qiming Li,[†] Jingfei Zhang,[†] Lili Zhang,[†] and Tian Wang[†,1]

[†]College of Animal Sciences and Technology, Nanjing Agricultural University, Nanjing, Jiangsu, P. R. China, 210095, [‡]College of Animal Science, Zhejiang University, Hangzhou, Zhejiang, P. R. China, 310000

[1]Corresponding author: tianwangnjau@163.com

ORCiD number: 0000-0002-9038-5009 (T. Wang).

Abstract

Few studies have focused on the role of dimethylglycine sodium (**DMG-Na**) salt in protecting the redox status of skeletal muscle, although it is reported to be beneficial in animal husbandry. This study investigated the beneficial effects of DMG-Na salt on the growth performance, longissimus dorsi muscle (**LM**) redox status, and mitochondrial function in weaning piglets that were intrauterine growth restricted (**IUGR**). Ten normal birth weight (**NBW**) newborn piglets (1.53 ± 0.04 kg) and 20 IUGR newborn piglets (0.76 ± 0.06 kg) from 10 sows were obtained. All piglets were weaned at 21 d of age and allocated to the three groups with 10 replicates per group: NBW weaned piglets fed a common basal diet (**N**); IUGR weaned piglets fed a common basal diet (**I**); IUGR weaned piglets fed a common basal diet supplemented with 0.1% DMG-Na (**ID**). They were slaughtered at 49 d of age to collect the serum and LM samples. Compared with the N group, the growth performance, LM structure, serum, and, within the LM, mitochondrial redox status, mitochondrial respiratory chain complex activity, energy metabolites, redox status-related, cell adhesion-related, and mitochondrial function-related gene expression, and protein expression deteriorated in group I ($P < 0.05$). The ID group showed improved growth performance, LM structure, serum, and, within the LM, mitochondrial redox status, mitochondrial respiratory chain complex activity, energy metabolites, redox status-related, cell adhesion-related, and mitochondrial function-related gene expression, and protein expression compared with those in the I group ($P < 0.05$). The above results indicated that the DMG-Na salt treatment could improve the LM redox status and mitochondrial function in IUGR weaned piglets via the nuclear factor erythroid 2-related factor 2/sirtuin 1/peroxisome proliferator-activated receptorγcoactivator-1α network, thus improving their growth performance.

Key words: dimethylglycine sodium salt, intrauterine growth restriction, longissimus dorsi muscle, mitochondrial dysfunction, redox status, weaned piglets

Abbreviations

8-OHdG	8-hydroxy-2-deoxyguanosine
ATP	adenosine triphosphate;
BCA	bicinchoninic acid
BWG	body weight gain
CAT	catalase
DCFH-DA	dichlorodihydrofluorescein diacetate
DMG-Na	dimethylglycine sodium
ETC	electron transport chain
FBW	final body weight
FI	feed intake
G:F	feed conversion ratio
GR	glutathione reductase
GSH	glutathione
GSH-Px	glutathione peroxidase
IBW	initial body weight
IUGR	intrauterine growth restriction
LM	longissimus dorsi muscle
MMP	mitochondrial membrane potential
mtDNA	mitochondrial DNA
NAD+	nicotinamide adenine dinucleotide
NBW	normal birth weight
PC	protein carbonyls
qPCR	quantitative real-time polymerase chain reaction
ROS	reactive oxygen species
SOD	superoxide dismutase

Introduction

Intrauterine growth restriction (**IUGR**), defined as being small for gestational age with weight below the 10th percentile or the population mean minus two SDs of a population-based nomogram, is an important problem in animal husbandry (Zhang et al., 2019). IUGR weaned piglets suffer from a permanent stunting effect due to lack of efficient nutrient utilization and impaired long-term health because of inadequate food intake, disease, or oxidative stress (Dong et al., 2016). Skeletal muscle mitochondrial dysfunction is associated with growth restriction and metabolic disorders at various periods of life. However, little is known about the postnatal effects of IUGR on the structure and function of the longissimus dorsi muscle (**LM**). This point appears to be important because the LM skeletal muscle has a lower priority for nutrient redistribution, which makes it particularly susceptible to nutritional deficiency in utero (JafariNasabian et al., 2017). After birth, slow skeletal muscle growth may, therefore, contribute to slow postnatal growth rates in neonates with IUGR, and the altered redox status and mitochondrial function of the skeletal muscle may negatively affect the growth performance and daily activities of neonates with IUGR throughout postnatal development and later on in adulthood (Năstase et al., 2018; Posont et al., 2021).

Mitochondria are the principal energy sources of the cell that convert nutrients into energy through cellular respiration; therefore, compromised mitochondrial structure and function are associated with many diseases (Dillin et al., 2002). Nuclear factor erythroid 2-related factor 2 (**Nrf2**) is important for maintaining mitochondrial function by regulating mitochondrial respiratory chain activity and is also involved in the activation of the antioxidant network (Dinkova-Kostova and Abramov, 2015). Peroxisome proliferator-activated receptorγcoactivator-1α (**PGC1α**) is a coactivator with major pleiotropic functions in mitochondrial biogenesis, as it induces mitochondrial genes at the level of both the nuclear and mitochondrial genomes (Jornayvaz and Shulman, 2010). Its activity is downregulated, followed by elevated reactive oxygen species (**ROS**), which is induced by oxidative damage and results in the activation of both enzymatic and nonenzymatic antioxidant defenses (St-Pierre et al., 2006). Sirtuin 1 (**SIRT1**), originally described as a factor regulating apoptosis and DNA repair, is highly sensitive to the cellular redox status and is known to control genomic stability and cellular metabolism (Tang, 2016). Previous studies have suggested that SIRT1 physically interacts with and deacetylates PGC1α at multiple lysine sites, thus increasing PGC1α activity and influencing the redox status (Aquilano et al., 2013).

Dimethylglycine sodium (**DMG-Na**) salt can improve the body's redox status and relieve oxidative damage by scavenging excessive free radicals. This is because it is similar to choline and betaine and is an important material for the synthesis of glutathione (Friesen et al., 2007b). Previous studies indicated that DMG-Na could improve the utilization of oxygen, thus protecting the body against the oxidative damage. It also enhanced the immune response of individuals, thereby improving their body performance (Bai et al., 2019). In this study, decreased SIRT1 activity impaired the LM redox status and mitochondrial function via its substrate PGC1α, thus decreasing the performance of IUGR weaned piglets. We also provide a novel insight into the effects of DMG-Na salt on the growth performance, LM redox status, and mitochondrial function in IUGR weaned piglets via the Nrf2/SIRT1/PGC1α network.

Materials and Methods

This trial was conducted in accordance with the Chinese guidelines for animal welfare and the experimental protocols for animal care approved by the Nanjing Agricultural University Institutional Animal Care and Use Committee (SYXK(Su)2017-0027).

Animal experiment and sampling

This experiment was conducted on a trial pig farm that was owned by the Yangzhou Fangling Agricultural and Pastoral Co., Ltd. (Jiangsu, China). A total of 80 healthy pregnant multiparous sows (Landrace × Yorkshire) with similar expected farrowing dates (less than 3 d) and parity (second or third) were preselected during gestation. The sows were fertilized by the pool of Duroc boars and fed the same gestating diet that met the National Research Council (NRC, 2012) nutrient requirements. At farrowing, 10 sows that had 11 to 13 live-born piglets and met the selection criteria for IUGR were chosen. Piglets with birth weights of 1.53 ± 0.04 and 0.76 ± 0.06 kg (mean ± SEM) in this work were selected as normal birth weight (**NBW**) newborn piglets and IUGR newborn piglets according to the method described by Wang et al. (2005), respectively. In each litter, one NBW and two IUGR newborn piglets were obtained. The piglets were weaned at 21 d of age and assigned to three groups with 10 replicates per group: The NBW piglets were allocated to the **N** group that fed a common basal diet (Supplementary Table S1), and the two IUGR piglets from one litter were randomly assigned to the **I** group that fed a common basal diet and **ID** group that fed a common basal diet supplemented with 0.1% DMG-Na salt (99.9% of purity, Qilu Shenghua Pharmaceutical Co., Ltd., Shandong, China). The piglets were housed individually in plastic floored pens (1 × 0.6 m) at an ambient temperature of 28 °C in an environmentally controlled room and had free access to water.

At 49 d of age, all piglets were weighed after feed deprivation for 12 h, and the initial body weight (**IBW**), final body weight

(**FBW**), feed intake (**FI**), and feed conversion ratio (**G:F**) values were calculated. The blood samples were withdrawn from the precaval vein, and the serum samples were separated by centrifugation at 3,500 × *g* for 15 min at 4 °C, and then stored at –80 °C until analysis. After blood sampling, the piglets were anesthetized via electrical stunning and sacrificed by exsanguination. Subsequently, the LM samples were harvested immediately: one (1 × 1 × 1 cm) sample for the morphological measurements embedded into 4% buffered formaldehyde solution and another sample storied at –80 °C for further study.

Morphological measurements of the LM

The LM samples fixed in 4% buffered formaldehyde were dried using a graded series of xylene and ethanol and then embedded into paraffin for histological processing. The samples (8 μm in size) were deparaffinized using xylene and rehydrated with graded dilutions of ethanol. The slides were stained with hematoxylin and eosin. Ten slides for each sample (the middle site of samples) were prepared, and the images were acquired using an optical binocular microscope (Cheng et al., 2020).

Redox status examination

The LM sample was homogenized in 0.9% sodium chloride solution on ice and centrifuged at 3,500 × *g* for 15 min at 4 °C. The serum and supernatant were individually used to measure the levels of superoxide dismutase (**SOD**), glutathione peroxidase (**GSH-Px**), GSH, glutathione reductase (**GR**), and catalase (**CAT**) using the corresponding assay kit following the manufacturer's instructions (Nanjing Jiancheng Institute of Bioengineering, Jiangsu, China) (Paglia and Valentine, 1967; Nozik-Grayck et al., 2005; Heras et al., 2018). The protein content was determined using a bicinchoninic acid (**BCA**) protein assay kit according to the manufacturer's instructions (Nanjing Jiancheng Institute of Bioengineering, Jiangsu, China).

Mitochondrial redox status measurement

The mitochondria of the LM samples were obtained according to the method described by Roediger and Truelove (1979). The levels of MnSOD, GSH-Px, GSH, GR, and γ-glutamylcysteine ligase (**γ-GCL**) in the LM mitochondria were calculated using an assay kit according to the manufacturer's instructions (Nanjing Jiancheng Institute of Bioengineering, Jiangsu, China; Paglia and Valentine, 1967; Nozik-Grayck et al., 2005; Heras et al., 2018).

Oxidative damage measurement

The ROS level was detected using a ROS assay kit (Nanjing Jiancheng Institute of Bioengineering; Sang et al., 2012). Briefly, the mitochondria were incubated with 10 μM of dichlorodihydrofluorescein diacetate (**DCFH-DA**) and 10 mmol/L of DNA stain Hoechst 33342 at 37 °C for 30 min. Then, the DCFH fluorescence of the mitochondria was measured at an emission wavelength of 530 nm and an excitation wavelength of 485 nm with a fluorescence reader (FACS Aria III; BD Biosciences, Franklin Lakes, NJ, USA). The results were expressed as the mean DCFH-DA fluorescence intensity over that of the control.

The mitochondrial membrane potential (**MMP**) level was calculated according to a method described by Zhang et al. (2011). Briefly, the mitochondria were loaded with 1 × JC-1 dye at 37 °C for 20 min and then analyzed, after washing, by flow cytometry (FACS Aria III). The MMP was calculated as the increase in the ratio of green and red fluorescence. The results were calculated as the ratio of the fluorescence of aggregates (red) to that of the monomers (green).

The number of apoptotic and necrotic cells was measured by an Alexa Fluor 488 Annexin V/dead Cell Apoptosis kit (Thermo Fisher Scientific, Inc., Waltham, MA, USA). Briefly, the LM samples were grinded by a glass homogenizer grinding, and their cells were washed twice with cool phosphate-buffered saline (PBS) buffer (pH = 7.4) and resuspended (2% suspension) in 1 × Annexin-binding buffer. Then, the cell density was determined and diluted in 1 × Annexin-binding buffer to 1 × 10^6 cells/mL. A sufficient volume of the above cell suspension was stained with Annexin V-fluorescein isothiocyanate and propidium iodide (1:9 dilution) staining solution in dark for 15 min at room temperature. After incubation, the forward scatter of cells was determined, and Annexin V fluorescence intensity was measured in FL-1 with 488 nm excitation wavelength and 530 nm emission wavelength on a FACS caliber (BD Biosciences).

Malondialdehyde in the LM sample was calculated using a malondialdehyde assay kit following the manufacturer's instructions (Nanjing Jiancheng Institute of Bioengineering, Jiangsu, China). Protein carbonyls (**PC**) and 8-hydroxy-2-deoxyguanosine (**8-OHdG**) in the LM sample were calculated using their respective enzyme-linked immunosorbent assay (ELISA) kits following the manufacturer's instructions (Nanjing Jiancheng Institute of Bioengineering, Jiangsu, China) (Valavanidis et al., 2009; Bai et al., 2011).

Mitochondrial electron transport chain complexes examination

The electron transport chain (**ETC**) complexes I, II, III, IV, and V activities of the LM sample were measured using an ELISA kit according to the manufacturer's instructions (SinoBestBio, Shanghai, China; Sousa et al., 2018).

Energy metabolites examination

The glycogen content in the LM samples was measured using a commercial kit (Nanjing Jiancheng Institute of Bioengineering, Nanjing, China; Ørtenblad et al., 2013). The concentrations of nicotinamide adenine dinucleotide (**NAD^+**) and nicotinamide adenine dinucleotide cofactor (NADH) in the LM samples were determined using commercial kits according to the manufacturer's instructions (SinoBestBio, Shanghai, China; Elhassan et al., 2019). The adenosine triphosphate (**ATP**) content in the LM sample was determined using an ATP Assay Kit (Solarbio, Beijing, China) following the manufacturer's instructions (Zhang et al., 2014).

The mitochondrial DNA (**mtDNA**) copy number of the LM sample was determined (Grady et al., 2018) using a real-time fluorescence quantitative polymerase chain reaction (**qPCR**) kit (Tli RNaseH Plus; Takara Bio, Inc., Otsu, Japan). In brief, the 20 μL PCR mixture consisted of 10 μL of SYBR Premix Ex Taq (2X), 0.4 μL of upstream primer, 0.4 μL of downstream primer, 0.4 μL of ROX dye (50X), 6.8 of μL ultra-pure water, and 2 μL of complementary DNA (cDNA) template. The sequence of the Mt D-loop gene upstream primer was 5′-AGGACTACGGCTTGAAAAGC-3′ and that of the downstream primer was 5′-CATCTTGGCA TCTTCAGTGCC-3′; the length of the target fragment was 198 bp. The sequence of the β-actin upstream primer was 5′-TTCTTGGGTATGGAGTCCTG-3′ and that of the downstream primer was 5′-TAGAAGCATTTGCGGTGG-3′; the length of the target fragment was 150 bp. The amplification of each LM sample was performed in triplicate. The fold expression of each gene was calculated according to the $2^{-\Delta\Delta Ct}$ method (Mohamed et al., 2010), in which β-actin was used as an internal standard.

RNA extraction and quantitative real-time polymerase chain reaction

Quantitative real-time PCR was performed as previously described (Mohamed et al., 2010). Total RNA was obtained from the LM sample using Trizol Reagent (TaKaRa, Dalian, China) and then reverse-transcribed using a commercial kit (Perfect Real Time, SYBR® PrimeScript, TaKaRa) following the manufacturer's instructions. The mRNA expression levels of specific genes were quantified via real-time PCR using SYBR® *Premix Ex Taq* II (Tli RNaseH Plus) and an ABI 7300 Fast Real-Time PCR detection system (Applied Biosystems, Foster City, CA). The SYBR Green PCR reaction mixture consisted of 10 μL SYBR® *Premix Ex Taq* (2X), 0.4 μL of the forward and reverse primers, 0.4 μL of ROX reference dye (50X), 6.8 μL of ddH_2O, and 2 μL of cDNA template. Each sample was amplified in triplicate. The fold expression of each gene was calculated according to the $2^{-\Delta\Delta Ct}$ method (Mohamed et al., 2010), in which the β-*actin* gene was used as an internal standard. The primer sequences used are presented in Supplementary **Table S2**.

Western blotting examination

Total protein was isolated from the three LM samples per group with a radioimmunoprecipitation assay lysis buffer containing protease inhibitor cocktail (Beyotime Institute of Biotechnology, Jiangsu, China). The nuclear protein in the LM samples was carried out using a Nuclear Protein Extraction Kit (Beyotime Institute of Biotechnology, Jiangsu, China). The concentrations of total cellular protein and nuclear protein in the LM samples were measured by the BCA protein assay kit (Beyotime Institute of Biotechnology, Jiangsu, China). Antibodies against related proteins were all purchased from Cell Signaling Technology (Danvers, MA, USA). Thereafter, equal quantities of protein were resolved by sodium dodecyl sulfate (SDS)-PAGE gel and then transferred onto polyvinylidene difluoride membranes. After that, the membranes were incubated with blocking buffer (5% bovine serum albumin in Tris-buffered saline containing 1% Tween 20) for 1 h at room temperature and probed with the primary antibody (1:1,000) against Nrf2 (# 12721S), heme oxygenase 1 (HO1; # 82206S), SOD (# 37385S), GSH-Px (# 3286S), Sirt1 (# 9475S), PGC1α (# 2178S), cytochrome C (Cyt C; # 11940S), estrogen-related receptor α (ERRα; # 13826S), mitochondrial transcription factor A (mtTFA; # 8076S), Tubulin (# 2125S) overnight at 4 °C. Then, the membranes were washed by Tris-buffered saline with 0.05% Tween 20 and incubated with a suitable secondary antibody for 1 h at room temperature. Finally, the blots were detected using enhanced chemiluminescence reagents (ECL-Kit, Beyotime, Jiangsu, China), followed by autoradiography. Photographs of the membranes were taken using the Luminescent Image Analyzer LAS-4000 system (Fujifilm Co.) and quantified with ImageJ 1.42 q software (NIH, Bethesda, MD, USA).

Statistical analysis

Data are presented as the mean ± SEM and were analyzed by a one-way analysis of variance procedure in Statistical Analysis System software (version 9.1; SAS Institute, Inc., Cary, NC, USA). This was followed by a Tukey's test when significant differences were found. Statistical significance was considered at $P < 0.05$. Thirty weaned piglets were evaluated at least three times for each assay.

Results

Growth performance

The protective effects of DMG-Na salt on the growth performance of IUGR weaned piglets are presented in Table 1. Compared with the N group, the I group showed significantly lower IBW, FBW, body weight gain (**BWG**), and FI values ($P < 0.05$). The FBW, BWG, and G:F values of the ID group were significantly improved compared with those in the I group ($P < 0.05$).

Morphological measurements of the LM

The protective effects of DMG-Na salt on the LM structure of IUGR weaned piglets are shown in Figure 1. Compared with the N group, internal structure damage and larger intercellular space were observed in group I, and these features were not found in the N group. The internal structure and intercellular space of the ID group were improved compared with those of the I group.

Redox status examination

The protective effects of DMG-Na salt on the serum and LM redox status of IUGR weaned piglets are shown in Figure 2. Compared with the N group, the I group showed significantly lower SOD, GSH-Px, GSH, GR, and CAT activity ($P < 0.05$). The SOD, GSH-Px, GSH, GR, and CAT activities of the ID group were significantly improved compared with those of the I group ($P < 0.05$).

Mitochondrial redox status measurement

The protective effects of DMG-Na salt on the mitochondrial redox status of IUGR weaned piglets are shown in Figure 3. Compared with the N group, the I group showed a significant decrease in the LM MnSOD, GSH-Px, GSH, GR, and γ-GCL activity ($P < 0.05$). The LM mitochondrial MnSOD, GSH-Px, GSH, GR, and γ-GCL activity of the ID group were all significantly improved compared with those in the I group ($P < 0.05$).

Oxidative damage measurement

The protective effects of DMG-Na on the LM oxidative damage of IUGR weaned piglets are shown in Figure 4. Compared with the N group, significantly higher levels of ROS, PC, 8-OHdG, apoptosis, and necrosis ($P < 0.05$) and significantly lower MMP levels ($P < 0.05$) were observed in the group I. Significantly decreased levels of ROS, PC, 8-OHdG, apoptosis, and necrosis ($P < 0.05$) and significantly increased MMP levels ($P < 0.05$) were observed in the ID group compared with the respective values in the group I.

Mitochondrial ETC complexes examination

The protective effects of DMG-Na salt on the mitochondrial ETC complexes of the IUGR weaned piglets are presented in Table 2. The I group showed a significantly lower level of LM complex I and complex V with respect to their levels in the N

Table 1. The growth performance of the IUGR weaned piglets fed diet supplemented with DMG-Na salt[1]

Item	Treatment		
	N	I	ID
IBW, kg	7.71 ± 0.58[a]	5.80 ± 0.60[b]	6.02 ± 0.57[b]
FBW, kg	17.04 ± 1.22[a]	13.74 ± 1.12[c]	15.87 ± 2.02[b]
BWG, kg	9.33 ± 1.05[a]	7.94 ± 0.88[b]	9.85 ± 1.63[a]
FI, kg	17.00 ± 1.07[a]	14.90 ± 0.96[b]	15.30 ± 1.05[b]
G:F[2]	0.55 ± 0.04[b]	0.53 ± 0.06[b]	0.64 ± 0.05[a]

[1]Data are presented as the mean ± SEM, $n = 10$ piglets/group.
[2]G:F, body weight gain: feed intake.
[a–c]Data in the same row with different superscripts were significantly different ($P < 0.05$).

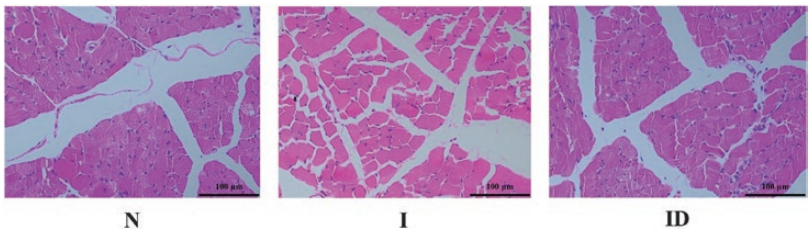

Figure 1. The LM morphological of the IUGR weaned piglets fed diet supplemented with DMG-Na salt. The LM morphological (internal structure and intercellular space) was scanned. Scale bars represent 100 μm.

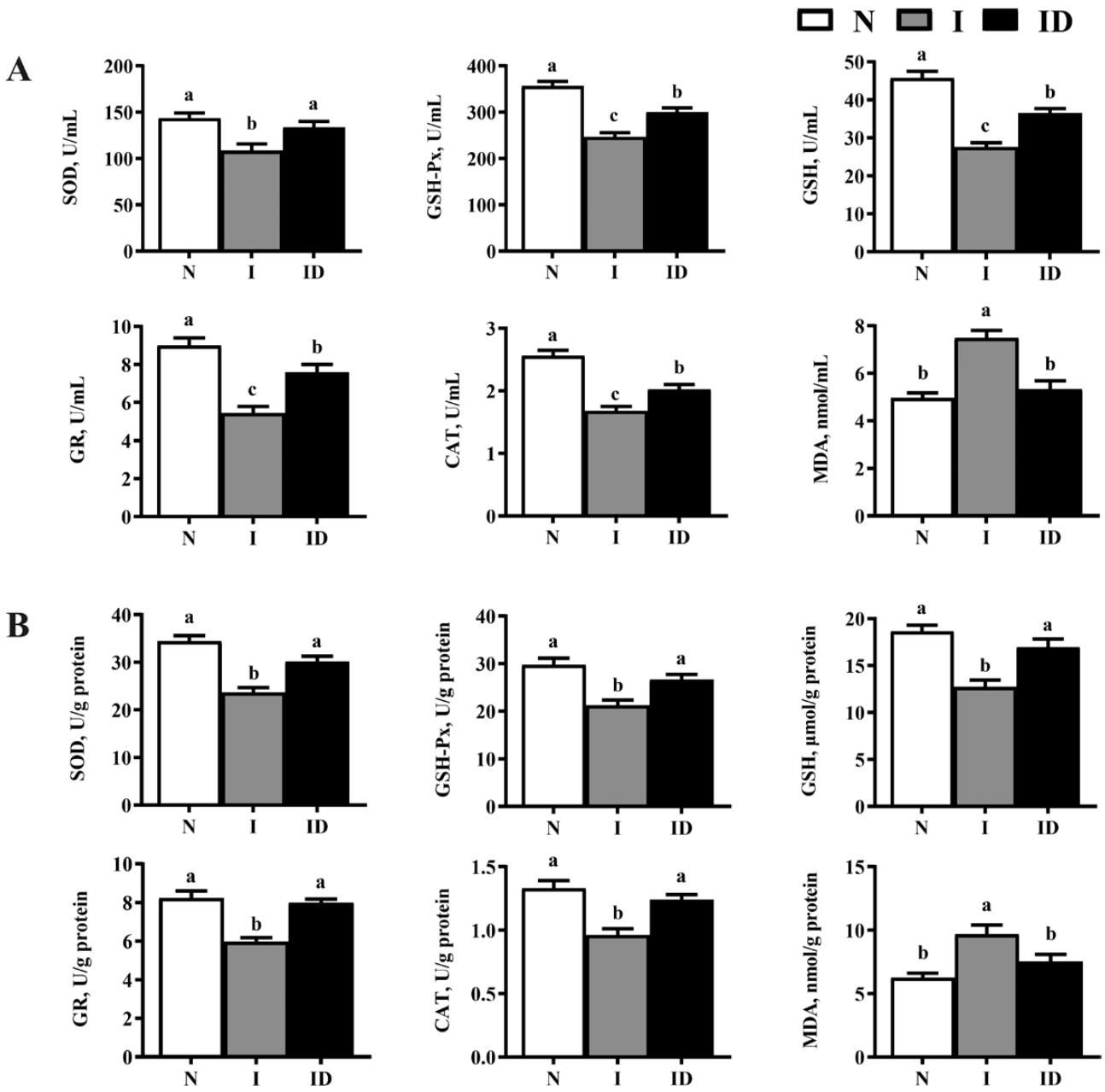

Figure 2. The serum (A) and LM (B) redox status of the IUGR weaned piglets fed diet supplemented with DMG-Na salt. Data are presented as the mean (n = 10 piglets/group) with their SEs represented by vertical bars. Groups with different superscripts were significantly different ($P < 0.05$). All the experiment was repeated three times.

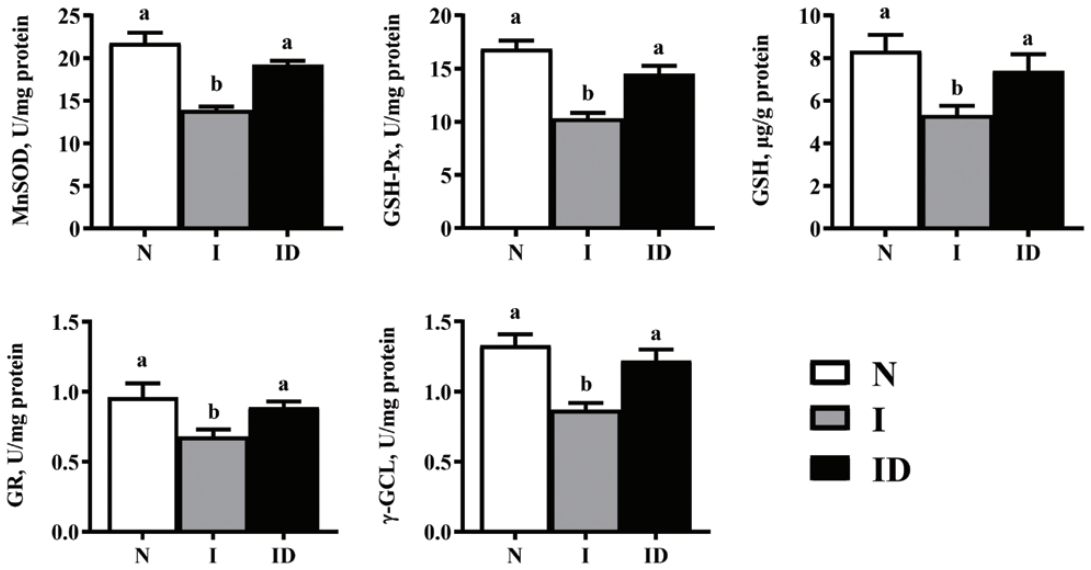

Figure 3. The LM mitochondrial redox status of the IUGR weaned piglets fed diet supplemented with DMG-Na salt. Data are presented as the mean (n = 10 piglets/group) with their SEs represented by vertical bars. Groups with different superscripts were significantly different ($P < 0.05$). All the experiment was repeated three times.

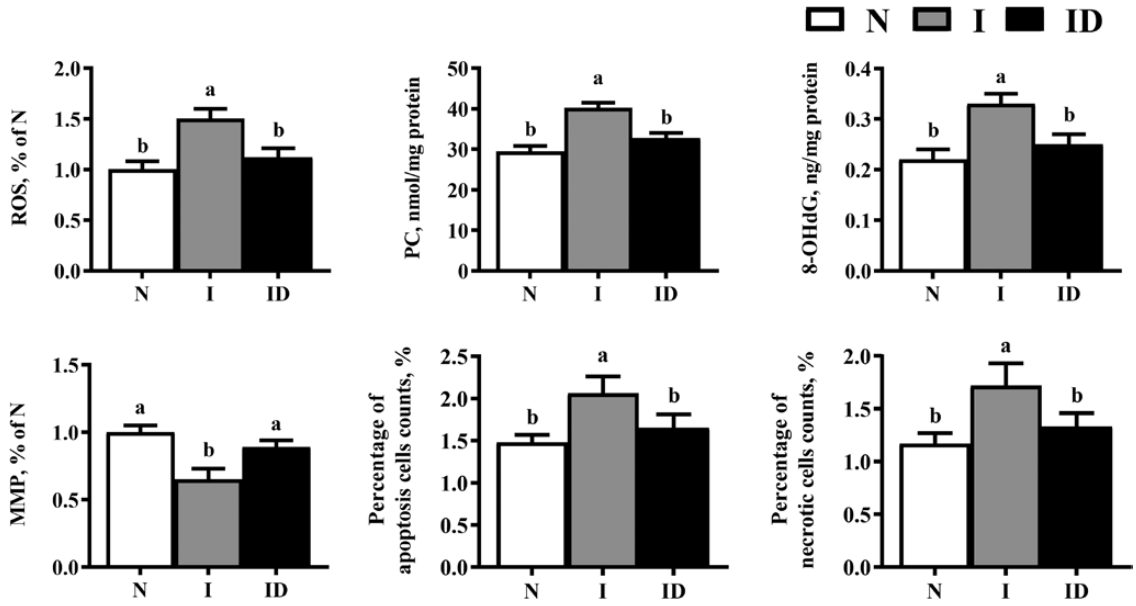

Figure 4. The LM oxidative damage of the IUGR weaned piglets fed diet supplemented with DMG-Na salt. Data are presented as the mean (n = 10 piglets/group) with their SEs represented by vertical bars. Groups with different superscripts were significantly different ($P < 0.05$). All the experiment was repeated three times.

group ($P < 0.05$). Compared with the I group, the ID group showed significantly higher levels of LM complex I and complex V ($P < 0.05$).

Energy metabolites examination

The protective effects of DMG-Na salt on the LM energy metabolism of IUGR weaned piglets are presented in Table 3. Compared with the N group, significantly higher levels of NADH ($P < 0.05$) and lower levels of glycogen, NAD^+, NAD^+/NADH, and ATP ($P < 0.05$) were observed in the group I. Significantly decreased levels of NADH ($P < 0.05$) and increased levels of glycogen, NAD^+, NAD^+/NADH, and ATP ($P < 0.05$) were observed in the ID group compared with the respective values in the group I.

Gene expression

The protective effects of DMG-Na salt on LM redox status-related and mitochondrial function-related gene expression in IUGR weaned piglets are shown in Figure 5. The redox status-related (*Nrf2*, *HO1*, *Cu/ZnSOD*, *GSH-Px*, *MnSOD*, *γ-GCLc*, *γ-GCLm*, thioredoxin 2 [*Trx2*], thioredoxin reductase 2 [*Trx-R2*], peroxiredoxin 3 [*Prx3*], *Sirt1*, *PGC1α*) gene expression, cell adhesion-related (occluding [*OCLN*], cloudin [*CLDN*] 2, *CLDN3*, and zonula occludens-1 [*ZO1*]) genes expression, and mitochondrial function-related (malonyl-CoA decarboxylase [*MCD*], medium-chain acyl-CoA dehydrogenase [*MCAD*], succinate dehydrogenase [*SDH*], uncoupling protein 2 [*UCP2*], cyclooxygenase 2 [*COX2*], citrate synthase [*CS*], cyclooxygenase 1 [*COX1*], *Cyt C*, *ERRα*, major histocompatibility complex I [*MHC1*],

Table 2. The LM mitochondrial ETC complexes of the IUGR weaned piglets fed diet supplemented with DMG-Na salt[1]

Item, nmol/min/mg protein	Treatment		
	N	I	ID
Complex I	254.22 ± 9.03[a]	215.72 ± 8.03[b]	242.77 ± 7.56[a]
Complex II	2.62 ± 0.45	2.01 ± 0.21	2.54 ± 0.33
Complex III	33.50 ± 0.89	25.21 ± 1.15	28.15 ± 1.21
Complex IV	15.20 ± 0.65	12.54 ± 0.71	13.21 ± 0.56
Complex V	47.38 ± 1.62[a]	36.57 ± 1.57[b]	44.65 ± 1.46[a]

[1]Data are presented as the mean ± SEM, n = 10 piglets/group.
[a,b]Data in the same row with different superscripts were significantly different ($P < 0.05$).

Table 3. The LM energy metabolism of the IUGR weaned piglets fed diet supplemented with DMG-Na salt1

Item	Treatment		
	N	I	ID
ATP, nmol/g	172.41 ± 8.09[a]	112.77 ± 6.21[b]	166.76 ± 6.38[a]
mtDNA, % of N	1.00 ± 0.13[a]	0.61 ± 0.09[b]	0.88 ± 0.08[a]
Glycogen, mg/g	72.52 ± 2.03[a]	52.44 ± 1.51[b]	69.78 ± 1.36[a]
NAD^+, μmol/g	2.38 ± 0.21[a]	1.21 ± 0.16[b]	1.92 ± 0.20[a]
NADH, μmol/g	0.99 ± 0.07[b]	1.39 ± 0.10[a]	0.71 ± 0.05[b]
NAD^+/NADH	2.40 ± 0.12[a]	0.87 ± 0.07[b]	2.70 ± 0.20[a]

[1]Data are presented as the mean ± SEM, n = 10 piglets/group.
[a,b]Data in the same row with different superscripts were significantly different ($P < 0.05$).

mtTFA, NADH dehydrogenase (ubiquinone) iron-sulfur protein 2 [*Ndufa2*], nuclear respiratory factor 1 [*NRF1*], uncoupling protein 1 [*UCP1*], γ DNA polymerases catalytic subunit γ [*POLG1*], DNA polymerases accessory subunit [*POLG2*], single-strand DNA-binding protein 1 [*SSBP1*], dynamin-related protein 1 [*Drp1*], mitochondrial fission 1 [*Fis1*], and mitochondrial mitofusin2 [*Mfn2*]) gene expression of the LM significantly deteriorated more in the group I than in the group N ($P < 0.05$). Compared with the I group, redox status-related gene expression, cell adhesion-related gene expression, and mitochondrial function-related gene expression of the LM were significantly improved in the ID group ($P < 0.05$).

Protein expression

The protective effects of DMG-Na salt on LM redox status-related protein expression and mitochondrial function-related protein expression of IUGR weaned piglets are shown in Figure 6. Compared with the N group, the I group showed significantly lower SOD, GSH-Px, Sirt1, PGC1α, Cyt C, ERRα, and mtTFA contents ($P < 0.05$) along with higher Nrf2 and HO1 contents ($P < 0.05$). The ID group presented a significantly higher Sirt1 content ($P < 0.05$) and lower Nrf2 and HO1 contents ($P < 0.05$) as compared with the I group.

Discussion

IUGR is an important issue in the animal industry because it causes irreversible oxidative damage, delayed postnatal growth, and affects skeletal muscle health (JafariNasabian et al., 2017). Some studies have used IUGR weaned piglets as a model to exhibit poor performance (Wu et al., 2006; Amdi et al., 2016), and these outcomes agree with the current work that piglets with birth weights of 1.53 ± 0.04 and 0.76 ± 0.06 kg (mean ± SEM) were selected as NBW newborn piglets and IUGR newborn piglets, respectively. Skeletal muscle is the main component of the total body mass that absorbs circulatory glucose, synthesizes glycogen, is responsible for metabolic homeostasis, and is thus easily affected by oxidative damage (Davis et al., 2008). In this work, supplementation with DMG-Na salt could improve the growth performance of IUGR weaned piglets as compared with those of NBW weaned piglets; however, this still requires further study.

Oxidative damage could increase the ROS content, thus influencing the redox status and destroying the mitochondrial structure and function. This could be improved by SOD, which catalyzes the conversion of endogenous superoxide anions to hydrogen peroxide through disproportionation, and is finally neutralized by intracellular CAT and GSH-Px (Avci et al., 2012). Meanwhile, MnSOD, GSH, GR, and γ-GCL are crucial for suppressing oxidative damage in mitochondria (Langston et al., 2011). Previous studies found that DMG-Na salt could act as an antioxidant additive to improve the redox status of the body, thus relieving the oxidative damage induced by excessive ROS generation (Friesen et al., 2007a; Bai et al., 2016). In this work, consuming DMG-Na salt could be beneficial to the redox status by scavenging excessively generated ROS, thus maintaining the balance of the intracellular redox status. This may be one possible reason for the results observed in the histological analysis.

The ROS concentration in cells maintains a dynamic balance with the redox status system. However, this balance will be disturbed when subjected to oxidative stress (Sun and Zemel, 2009). Excessive ROS can induce mitochondrial and DNA structural damage and dysfunction, ultimately affecting the redox status (Sastre et al., 2000). IUGR is closely related to oxidative damage, mitochondrial dysfunction, high ROS levels, and the occurrence of metabolic syndrome (Rashid et al., 2018). It has been suggested that excessive ROS induces mtDNA damage, whereas impaired mitochondrial function produces more endogenous ROS (Simmons, 2012). The MMP level, which is negatively associated with ROS concentration, acts as an indicator at the beginning of mitochondria-dependent apoptosis (Kim and Kim, 2018). Consistent with this work, one study indicated that IUGR reduces the redox status of weaned piglets mainly due to the high ROS concentration (Park et al., 2004). Another study also found that IUGR piglets have reduced redox status and are prone to oxidative damage (Mert et al., 2012). It can be seen from the results that the reduction of the redox status in weaned piglets of the IUGR group leads to impaired skeletal muscle mitochondrial function. These results also suggested that DMG-Na salt could relieve oxidative damage due to excessive ROS generation, and different studies verified that natural antioxidants could protect cells from oxidative damage (Look et al., 2001). However, the effects of DMG-Na salt on reducing oxidative damage to skeletal muscle require further study.

Necessary for growth and glycogen synthesis and related to the mitochondrial number, ATP can be calculated quantitatively using the mtDNA copy number (Pinto and Moraes, 2015). A lower level of ATP in IUGR weaned piglets results in lower postnatal muscle growth and glycogen storage (Felicioni et al., 2020). The loss of complex I activity induced by oxidative damage in the LM mitochondria of IUGR weaned piglets could lead to a decrease in mitochondrial energy generation. In this work, the lower NAD^+/NADH ratio could

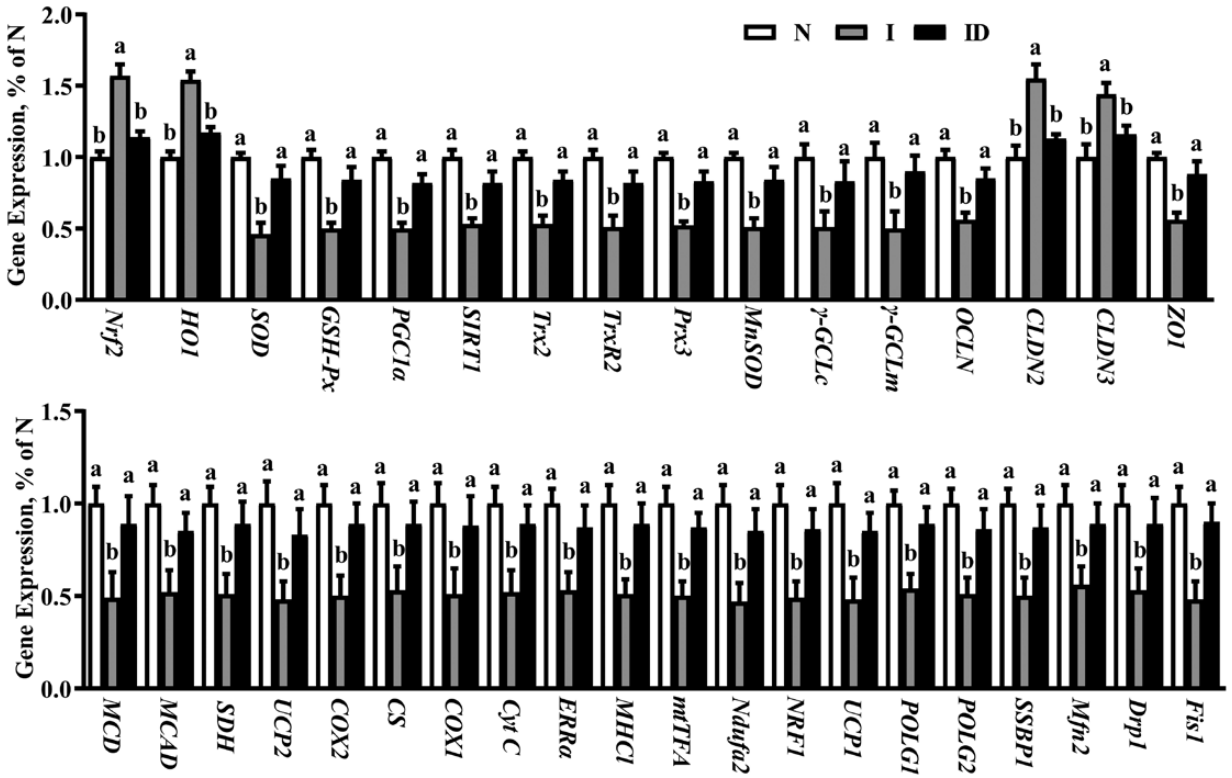

Figure 5. The LM gene expression of the IUGR weaned piglets fed diet supplemented with DMG-Na salt. Data are presented as the mean (n = 10 piglets/group) with their SEs represented by vertical bars. Groups with different superscripts were significantly different ($P < 0.05$). All the experiment was repeated three times.

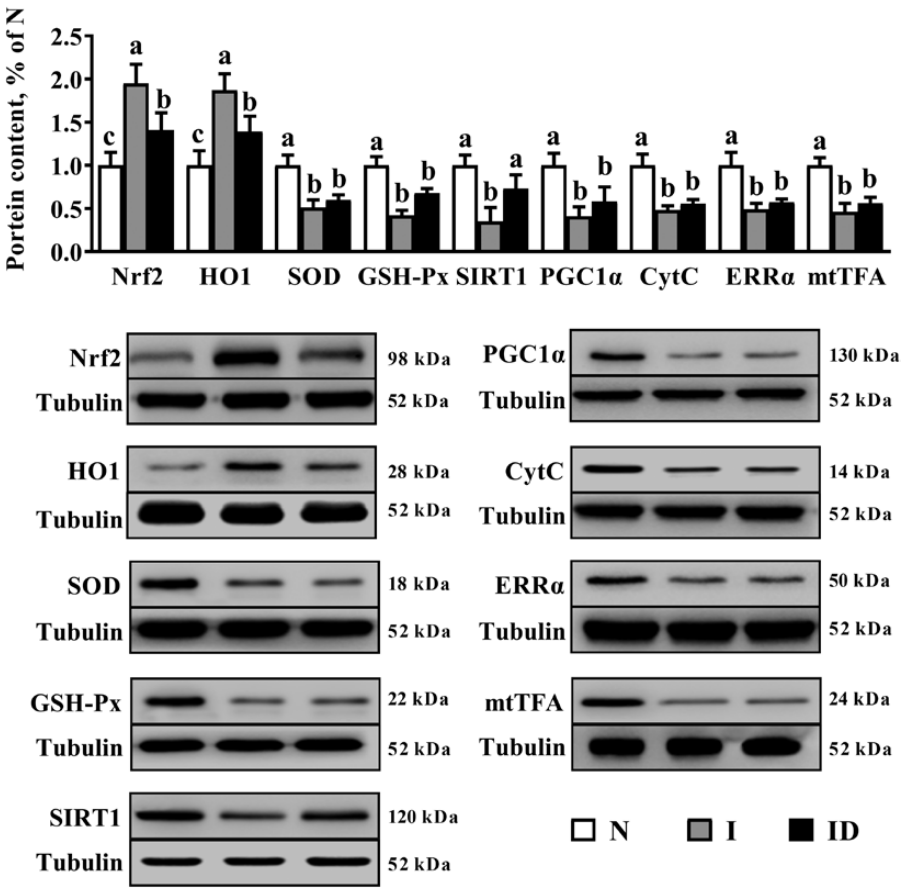

Figure 6. The LM protein expression of the IUGR weaned piglets fed diet supplemented with DMG-Na salt. Data are presented as the mean with their SEs represented by vertical bars. Groups with different superscripts were significantly different ($P < 0.05$). All the experiment was repeated three times.

be explained by the reduced activity of complex I, which couples electrons from NADH to quinone with the translocation of a proton across the inner mitochondrial membrane for ATP generation (Fiedorczuk and Sazanov, 2018). Moreover, it also inhibits the flux of glycolytic and tricarboxylic acid cyclic metabolites by the mitochondria, resulting in reduced ATP generation (Lane et al., 2001). An increase in complex V or ATP synthase activity in the LM mitochondria of IUGR weaned piglets is crucial in bioenergetics, which uses the exergonic proton backflow for ATP synthesis from ADP and inorganic phosphate in the matrix (Haraux and Lombès, 2019). A previous study suggested that DMG-Na salt acted as an antioxidant (Bai et al., 2019), thus protecting the skeletal muscle from oxidative damage and maintaining its normal structure and function. Another study found that DMG-Na salt exerted a beneficial effect on cells that protects them from oxidative damage (Zhang et al., 2014), and this might be one possible reason for the improvement of the LM mitochondrial ETC complex activity and energy metabolism level in the ID group.

The activation of Nrf2 and HO1 is important in relieving oxidative damage by regulating redox status-related gene expression (SOD, GSH-Px, and γ-GCL; Hwang et al., 2013). Mitochondria are rich in Trx2, Trx-R2, and Prx3 proteins, which act together to prevent oxidative damage by scavenging excessive free radicals and regulating mitochondria-dependent apoptotic pathways (Michelet et al., 2006). The protein PGC1α is a coactivator with pleiotropic functions that can regulate mitochondrial biogenesis (COX1, Cyt C, ERRα, MHC1, mtTFA, Ndufa2, NRF1, NRF2, and UCP1), mitochondrial function gene expression (mtDNA replication and repair [*POLG1*, *POLG2*, and *SSBP1*], mitochondrial fission [*Drp1* and *Fis1*], and fusion [*Mfn2*]), as it induces mitochondrial gene expression at the level of both the nuclear and mitochondrial genomes (Lin et al., 2005; St-Pierre et al., 2006). The factor SIRT1, originally described as a factor regulating apoptosis and DNA repair, is highly sensitive to cellular redox and nutritional status and is known to control genomic stability and cellular metabolism (Sinclair, 2005). Previous studies have reported that SIRT1 physically interacts with and deacetylates PGC1α at multiple lysine sites, consequently increasing the PGC1α activity and regulating the redox status, lipid oxidation enzymes (MCD and MCAD), and mitochondrial gene expression (*SDH*, *UCP2*, *COX2*, and *CS*) (Sinclair, 2005; Sánchez-Ramos et al., 2011). The factor ZO1, which is correlated with paracellular permeability, together with OCLN and CLDN are key regulators of cell permeability (Gu et al., 2011). To our knowledge, this is the first study to show the effects of DMG-Na salt on the LM redox status and mitochondrial function of IUGR weaned piglets via the Nrf2/SIRT1/PGC1α network, and further work is still needed to elucidate this specific mechanism.

In conclusion, this study demonstrated that DMG-Na salt could effectively reduce skeletal muscle structure damage and dysfunction in IUGR weaned piglets. We also found that DMG-Na salt could directly neutralize excessive free radicals and indirectly improve the redox status and inhibit the abnormal expression of stress-related factors via the Nrf2/SIRT1/PGC1α network. Therefore, this suggests that DMG-Na salt can serve as a health-promoting substance and can be used to treat skeletal muscle disorder in IUGR weaned piglets to improve their performance.

Supplementary Data

Supplementary data are available at *Journal of Animal Science* online.

Acknowledgments

This work was supported by the National Key Research and Development Program of China (2018YFD0501101) and the National Natural Science Foundation of China (N31802094).

Conflict of interest statement

No potential conflicts of interest relevant to this article were reported by the authors.

Literature Cited

Amdi, C., M. V. Klarlund, J. Hales, T. Thymann, and C. F. Hansen. 2016. Intrauterine growth-restricted piglets have similar gastric emptying rates but lower rectal temperatures and altered blood values when compared with normal-weight piglets at birth. *J. Anim. Sci.* **94**:4583–4590. doi:10.2527/jas.2016-0639

Aquilano, K., S. Baldelli, B. Pagliei, S. M. Cannata, G. Rotilio, and M. R. Ciriolo. 2013. p53 Orchestrates the PGC-1α-mediated antioxidant response upon mild redox and metabolic imbalance. *Antioxid. Redox Signal.* **18**:386–399. doi:10.1089/ars.2012.4615

Avci, G., H. Kadioglu, A. O. Sehirli, S. Bozkurt, O. Guclu, E. Arslan, and S. K. Muratli. 2012. Curcumin protects against ischemia/reperfusion injury in rat skeletal muscle. *J. Surg. Res.* **172**:e39–e46. doi:10.1016/j.jss.2011.08.021

Bai, P., C. Cantó, H. Oudart, A. Brunyánszki, Y. Cen, C. Thomas, H. Yamamoto, A. Huber, B. Kiss, R. H. Houtkooper, *et al.* 2011. PARP-1 inhibition increases mitochondrial metabolism through SIRT1 activation. *Cell Metab.* **13**:461–468. doi:10.1016/j.cmet.2011.03.004

Bai, K., L. Jiang, S. Zhu, C. Feng, Y. Zhao, L. Zhang, and T. Wang. 2019. Dimethylglycine sodium salt protects against oxidative damage and mitochondrial dysfunction in the small intestines of mice. *Int. J. Mol. Med.* **43**:2199–2211. doi:10.3892/ijmm.2019.4093

Bai, K., W. Xu, J. Zhang, T. Kou, Y. Niu, X. Wan, L. Zhang, C. Wang, and T. Wang. 2016. Assessment of free radical scavenging activity of dimethylglycine sodium salt and its role in providing protection against lipopolysaccharide-induced oxidative stress in mice. *PLoS One.* **11**:e0155393. doi:10.1371/journal.pone.0155393

Cheng, K., T. Wang, S. Li, Z. Song, H. Zhang, L. Zhang, and T. Wang. 2020. Effects of early resveratrol intervention on skeletal muscle mitochondrial function and redox status in neonatal piglets with or without intrauterine growth retardation. *Oxid. Med. Cell. Longev.* **2020**:4858975. doi:10.1155/2020/4858975

Davis, T. A., A. Suryawan, R. A. Orellana, H. V. Nguyen, and M. L. Fiorotto. 2008. Postnatal ontogeny of skeletal muscle protein synthesis in pigs. *J. Anim. Sci.* **86**(14 Suppl):E13–E18. doi:10.2527/jas.2007-0419

Dillin, A., A. L. Hsu, N. Arantes-Oliveira, J. Lehrer-Graiwer, H. Hsin, A. G. Fraser, R. S. Kamath, J. Ahringer, and C. Kenyon. 2002. Rates of behavior and aging specified by mitochondrial function during development. *Science* **298**:2398–2401. doi:10.1126/science.1077780

Dinkova-Kostova, A. T., and A. Y. Abramov. 2015. The emerging role of Nrf2 in mitochondrial function. *Free Radic. Biol. Med.* **88**(Pt B):179–188. doi:10.1016/j.freeradbiomed.2015.04.036

Dong, L., X. Zhong, J. He, L. Zhang, K. Bai, W. Xu, T. Wang, X. Huang. 2016. Supplementation of tributyrin improves the growth and intestinal digestive and barrier functions in intrauterine growth-restricted piglets. *Clin. Nutr.* **35**:399–407. doi:10.1016/j.clnu.2015.03.002

Elhassan, Y. S., K. Kluckova, R. S. Fletcher, M. S. Schmidt, A. Garten, C. L. Doig, D. M. Cartwright, L. Oakey, C. V. Burley, N. Jenkinson, *et al.* 2019. Nicotinamide riboside augments the

aged human skeletal muscle NAD(+) metabolome and induces transcriptomic and anti-inflammatory signatures. *Cell Rep.* **28**:1717–1728.e1716. doi:10.1016/j.celrep.2019.07.043

Felicioni, F., A. D. Pereira, A. L. Caldeira-Brant, T. G. Santos, T. M. D. Paula, D. Magnabosco, F. P. Bortolozzo, S. Tsoi, M. K. Dyck, W. Dixon, *et al.* 2020. Postnatal development of skeletal muscle in pigs with intrauterine growth restriction: morphofunctional phenotype and molecular mechanisms. *J. Anat.* **236**:840–853. doi:10.1111/joa.13152

Fiedorczuk, K., and L. A. Sazanov. 2018. Mammalian mitochondrial complex I structure and disease-causing mutations. *Trends Cell Biol.* **28**:835–867. doi:10.1016/j.tcb.2018.06.006

Friesen, R. W., E. M. Novak, D. Hasman, and S. M. Innis. 2007a. Relationship of dimethylglycine, choline, and betaine with oxoproline in plasma of pregnant women and their newborn infants. *J. Nutr.* **137**:2641–2646. doi:10.1093/jn/137.12.2641

Friesen, R. W., E. M. Novak, D. Hasman, and S. M. Innis. 2007b. Relationship of dimethylglycine, choline, and betaine with oxoproline in plasma of pregnant women and their newborn infants. *J. Nutr.* **137**:2641–2646. doi:10.1093/jn/137.12.2641

Grady, J. P., S. J. Pickett, Y. S. Ng, C. L. Alston, E. L. Blakely, S. A. Hardy, C. L. Feeney, A. A. Bright, A. M. Schaefer, G. S. Gorman, *et al.* 2018. mtDNA heteroplasmy level and copy number indicate disease burden in m.3243A>G mitochondrial disease. *EMBO. Mol. Med.* **10**(6):e8262. doi:10.15252/emmm.201708262

Gu, L., N. Li, J. Gong, Q. Li, W. Zhu, and J. Li. 2011. Berberine ameliorates intestinal epithelial tight-junction damage and down-regulates myosin light chain kinase pathways in a mouse model of endotoxinemia. *J. Infect. Dis.* **203**:1602–1612. doi:10.1093/infdis/jir147

Haraux, F., and A. Lombès. 2019. Kinetic analysis of ATP hydrolysis by complex V in four murine tissues: towards an assay suitable for clinical diagnosis. *PLoS One.* **14**:e0221886. doi:10.1371/journal.pone.0221886

Heras, R. L., J. L. Rodríguez-Gil, J. S. S. Sauto, P. S. Sánchez, and M. Catalá. 2018. Analysis of lipid peroxidation in animal and plant tissues as field-based biomarker in Mediterranean irrigated agroecosystems (Extremadura, Spain). *J. Environ. Sci. Health. B.* **53**:567–579. doi:10.1080/03601234.2018.1473962

Hwang, J. W., H. Yao, S. Caito, I. K. Sundar, and I. Rahman. 2013. Redox regulation of SIRT1 in inflammation and cellular senescence. *Free Radic. Biol. Med.* **61**:95–110. doi:10.1016/j.freeradbiomed.2013.03.015

JafariNasabian, P., J. E. Inglis, W. Reilly, O. J. Kelly, and J. Z. Ilich. 2017. Aging human body: changes in bone, muscle and body fat with consequent changes in nutrient intake. *J. Endocrinol.* **234**:R37–R51. doi:10.1530/JOE-16-0603

Jornayvaz, F. R., and G. I. Shulman. 2010. Regulation of mitochondrial biogenesis. *Essays Biochem.* **47**:69–84. doi:10.1042/bse0470069

Kim, S. H., and H. Kim. 2018. Inhibitory effect of astaxanthin on oxidative stress-induced mitochondrial dysfunction—a mini-review. *Nutrients* **10**(9):1137. doi:10.3390/nu10091137

Lane, R. H., D. E. Kelley, V. H. Ritov, A. E. Tsirka, and E. M. Gruetzmacher. 2001. Altered expression and function of mitochondrial beta-oxidation enzymes in juvenile intrauterine-growth-retarded rat skeletal muscle. *Pediatr. Res.* **50**:83–90. doi:10.1203/00006450-200107000-00016

Langston, J. W., W. Li, L. Harrison, and T. Y. Aw. 2011. Activation of promoter activity of the catalytic subunit of γ-glutamylcysteine ligase (GCL) in brain endothelial cells by insulin requires antioxidant response element 4 and altered glycemic status: implication for GCL expression and GSH synthesis. *Free Radic. Biol. Med.* **51**:1749–1757. doi:10.1016/j.freeradbiomed.2011.08.004

Lin, J., C. Handschin, and B. M. Spiegelman. 2005. Metabolic control through the PGC-1 family of transcription coactivators. *Cell Metab.* **1**:361–370. doi:10.1016/j.cmet.2005.05.004

Look, M. P., R. Riezler, H. K. Berthold, S. P. Stabler, K. Schliefer, R. H. Allen, T. Sauerbruch, and J. K. Rockstroh. 2001. Decrease of elevated N,N-dimethylglycine and N-methylglycine in human immunodeficiency virus infection during short-term highly active antiretroviral therapy. *Metabolism* **50**:1275–1281. doi:10.1053/meta.2001.27201

Mert, I., A. S. Oruc, S. Yuksel, E. S. Cakar, U. Buyukkagnici, A. Karaer, and N. Danisman. 2012. Role of oxidative stress in preeclampsia and intrauterine growth restriction. *J. Obstet. Gynaecol. Res.* **38**:658–664. doi:10.1111/j.1447-0756.2011.01771.x

Michelet, L., M. Zaffagnini, V. Massot, E. Keryer, H. Vanacker, M. Miginiac-Maslow, E. Issakidis-Bourguet, and S. D. Lemaire. 2006. Thioredoxins, glutaredoxins, and glutathionylation: new crosstalks to explore. *Photosynth. Res.* **89**:225–245. doi:10.1007/s11120-006-9096-2

Mohamed, J. S., M. A. Lopez, and A. M. Boriek. 2010. Mechanical stretch up-regulates microRNA-26a and induces human airway smooth muscle hypertrophy by suppressing glycogen synthase kinase-3β. *J. Biol. Chem.* **285**:29336–29347. doi:10.1074/jbc.M110.101147

Năstase, L., D. Cretoiu, and S. M. Stoicescu. 2018. Skeletal muscle damage in intrauterine growth restriction. *Adv. Exp. Med. Biol.* **1088**:93–106. doi:10.1007/978-981-13-1435-3_5

National Research Council (NRC). 2012. *Nutrient requirements of swine*. 11th ed. Washington (DC): National Academy Press.

Nozik-Grayck, E., H. B. Suliman, and C. A. Piantadosi. 2005. Extracellular superoxide dismutase. *Int. J. Biochem. Cell Biol.* **37**:2466–2471. doi:10.1016/j.biocel.2005.06.012

Ørtenblad, N., H. Westerblad, and J. Nielsen. 2013. Muscle glycogen stores and fatigue. *J. Physiol.* **591**:4405–4413. doi:10.1113/jphysiol.2013.251629

Paglia, D. E., and W. N. Valentine. 1967. Studies on the quantitative and qualitative characterization of erythrocyte glutathione peroxidase. *J. Lab. Clin. Med.* **70**:158–169.

Park, H. K., C. J. Jin, Y. M. Cho, D. J. Park, C. S. Shin, K. S. Park, S. Y. Kim, B. Y. Cho, and H. K. Lee. 2004. Changes of mitochondrial DNA content in the male offspring of protein-malnourished rats. *Ann. N. Y. Acad. Sci.* **1011**:205–216. doi:10.1007/978-3-662-41088-2_21

Pinto, M., and C. T. Moraes. 2015. Mechanisms linking mtDNA damage and aging. *Free Radic. Biol. Med.* **85**:250–258. doi:10.1016/j.freeradbiomed.2015.05.005

Posont, R. J., C. N. Cadaret, J. K. Beard, R. M. Swanson, R. L. Gibbs, E. S. Marks-Nelson, J. L. Petersen, and D. T. Yates. 2021. Maternofetal inflammation induced for two weeks in late gestation reduced birthweight and impaired neonatal growth and skeletal muscle glucose metabolism in lambs. *J. Anim. Sci.* **99**(5):skab102. doi:10.1093/jas/skab102

Rashid, C. S., A. Bansal, and R. A. Simmons. 2018. Oxidative stress, intrauterine growth restriction, and developmental programming of type 2 diabetes. *Physiology.* **33**:348–359. doi:10.1152/physiol.00023.2018

Roediger, W. E., and S. C. Truelove. 1979. Method of preparing isolated colonic epithelial cells (colonocytes) for metabolic studies. *Gut* **20**:484–488. doi:10.1136/gut.20.6.484

Sánchez-Ramos, C., A. Tierrez, O. Fabregat-Andrés, B. Wild, F. Sánchez-Cabo, A. Arduini, A. Dopazo, and M. Monsalve. 2011. PGC-1α regulates translocated in liposarcoma activity: role in oxidative stress gene expression. *Antioxid. Redox Signal.* **15**:325–337. doi:10.1089/ars.2010.3643

Sang, H., L. Zhang, and J. Li. 2012. Anti-benzopyrene-7,8-diol-9,10-epoxide induces apoptosis via mitochondrial pathway in human bronchiolar epithelium cells independent of the mitochondria permeability transition pore. *Food Chem. Toxicol.* **50**:2417–2423. doi:10.1016/j.fct.2012.04.041

Sastre, J., F. V. Pallardó, and J. Viña. 2000. Mitochondrial oxidative stress plays a key role in aging and apoptosis. *IUBMB Life* **49**:427–435. doi:10.1080/152165400410281

Simmons, R. A. 2012. Developmental origins of diabetes: the role of oxidative stress. *Best Pract. Res. Clin. Endocrinol. Metab.* **26**:701–708. doi:10.1016/j.beem.2012.03.012

Sinclair, D. A. 2005. Toward a unified theory of caloric restriction and longevity regulation. *Mech. Ageing Dev.* **126**:987–1002. doi:10.1016/j.mad.2005.03.019

Sousa, J. S., E. D'Imprima, and J. Vonck. 2018. Mitochondrial respiratory chain complexes. *Subcell. Biochem.* **87**:167–227. doi:10.1007/978-981-10-7757-9_7

St-Pierre, J., S. Drori, M. Uldry, J. M. Silvaggi, J. Rhee, S. Jäger, C. Handschin, K. Zheng, J. Lin, W. Yang, *et al.* 2006. Suppression of reactive oxygen species and neurodegeneration by the PGC-1 transcriptional coactivators. *Cell.* **127**:397–408. doi:10.1016/j.cell.2006.09.024

Sun, X., and M. B. Zemel. 2009. Leucine modulation of mitochondrial mass and oxygen consumption in skeletal muscle cells and adipocytes. *Nutr. Metab. (Lond).* **6**:26. doi:10.1186/1743-7075-6-26

Tang, B. L. 2016. Sirt1 and the mitochondria. *Mol. Cells* **39**:87–95. doi:10.14348/molcells.2016.2318

Valavanidis, A., T. Vlachogianni, and C. Fiotakis. 2009. 8-Hydroxy-2′-deoxyguanosine (8-OHdG): a critical biomarker of oxidative stress and carcinogenesis. *J. Environ. Sci. Health. C.* **27**:120–139. doi:10.1080/10590500902885684

Wang, T., Y. J. Huo, F. Shi, R. J. Xu, and R. J. Hutz. 2005. Effects of intrauterine growth retardation on development of the gastrointestinal tract in neonatal pigs. *Biol. Neonate* **88**:66–72. doi:10.1159/000084645

Wu, G., F. W. Bazer, J. M. Wallace, and T. E. Spencer. 2006. Board-Invited Review: Intrauterine growth retardation: implications for the animal sciences. *J. Anim. Sci.* **84**:2316–2337. doi:10.2527/jas.2006-156

Zhang, H., Y. Li, Y. Chen, L. Zhang, and T. Wang. 2019. *N*-acetylcysteine protects against intrauterine growth retardation-induced intestinal injury via restoring redox status and mitochondrial function in neonatal piglets. *Eur. J. Nutr.* **58**:3335–3347. doi:10.1007/s00394-018-1878-8

Zhang, J., L. Xu, L. Zhang, Z. Ying, W. Su, and T. Wang. 2014. Curcumin attenuates D-galactosamine/lipopolysaccharide-induced liver injury and mitochondrial dysfunction in mice. *J. Nutr.* **144**:1211–1218. doi:10.3945/jn.114.193573

Zhang, Q., P. Zou, H. Zhan, M. Zhang, L. Zhang, R. S. Ge, and Y. Huang. 2011. Dihydrolipoamide dehydrogenase and cAMP are associated with cadmium-mediated Leydig cell damage. *Toxicol. Lett.* **205**:183–189. doi:10.1016/j.toxlet.2011.06.003